

# We are IntechOpen, the world's leading publisher of Open Access books Built by scientists, for scientists

6,900

Open access books available

186,000

International authors and editors

200M

Downloads

Our authors are among the

154

Countries delivered to

TOP 1%

most cited scientists

12.2%

Contributors from top 500 universities



WEB OF SCIENCE™

Selection of our books indexed in the Book Citation Index  
in Web of Science™ Core Collection (BKCI)

Interested in publishing with us?  
Contact [book.department@intechopen.com](mailto:book.department@intechopen.com)

Numbers displayed above are based on latest data collected.  
For more information visit [www.intechopen.com](http://www.intechopen.com)



## Ferroelectric Liquid Crystals Composed of Banana-Shaped Thioesters

Stanisław Wróbel<sup>1</sup>, Janusz Chruściel<sup>2</sup>, Marta Wierzejska-Adamowicz<sup>1</sup>,  
Monika Marzec<sup>1</sup>, Danuta M. Ossowska-Chruściel<sup>2</sup>,  
Christian Legrand<sup>3</sup> and Redouane Douali<sup>3</sup>

<sup>1</sup>*Institute of Physics, Jagiellonian University, Kraków*

<sup>2</sup>*Institute of Chemistry, Siedlce University of Natural Sciences and Humanities, Siedlce*

<sup>3</sup>*Université du Littoral Côte d'Opale, LEMCEL, Calais*

<sup>1,2</sup>*Poland*

<sup>3</sup>*France*

### 1. Introduction

Thermotropic liquid crystals composed of rod like molecules are known as calamitic liquid crystals. Flatten molecules of some organic compounds form discotic liquid crystals. Both kinds of compounds may exhibit nematic phase. Calamitic mesogens may also form lamellar smectic structures being so important for living systems, whereas discotic molecules make columnar mesophases. Banana-shaped (bow-shaped or bent-core) ferroelectric liquid crystals have been discovered in the last decade of the 20-th century (Noiri et al., 1996). Since then there has been a great interest in their dielectric and electro-optic properties due to potential applications (Sekine et al., 1997; Link et al., 1997; Pelzl et al., 1999). At the beginning some of the bent-core compounds were not chemically stable enough as to study them experimentally during cooling and heating runs in long lasting experiments (Wróbel et al., 2000). It came out that bent-core achiral thioesters are very stable materials showing either B<sub>1</sub> or B<sub>2</sub> phase (Rouillon et al., 2001; Ossowska-Chruściel, 2007, 2009). In this article we present complementary studies on B<sub>1</sub> and B<sub>2</sub> phases of 1,3-phenylene bis{4-[4-alkoxybenzoyl]-sulfanyl}benzoates} (in short: nOSOR) having achiral symmetric bent-core molecules shown in Fig. 1.

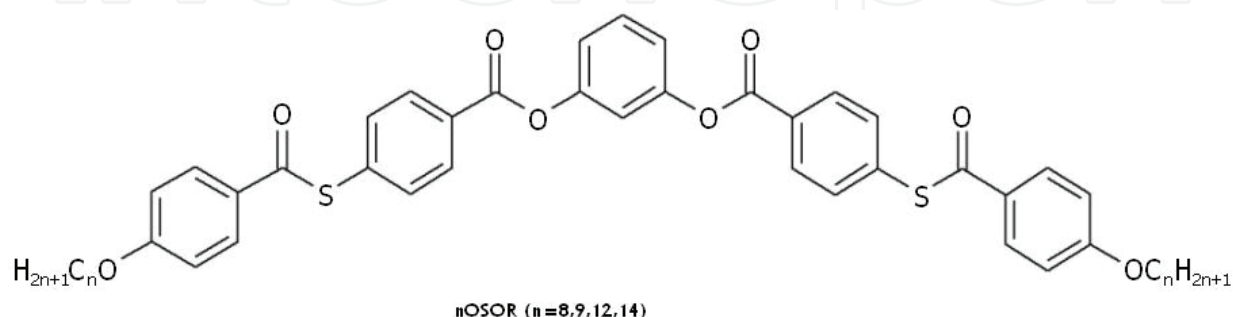


Fig. 1. Molecular structure of the symmetric thioester compounds studied

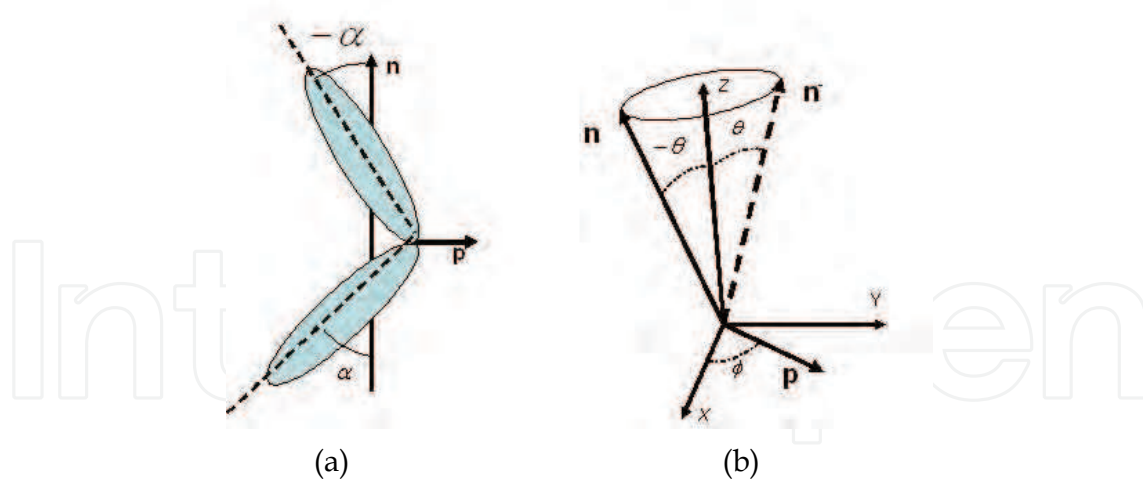


Fig. 2. (a) Simplified model of bent-core molecule and two directors  $n$  and  $p$ , (b) Primary  $n$  and secondary  $p$  directors in the  $(X,Y,Z)$  laboratory reference frame. In  $B_2$  phase the  $n$  director is tilted with respect to the smectic plane normal  $Z$  by the angle  $+\theta$  or  $-\theta$ . The  $n$  director is the average direction of the long molecular axis. The secondary director  $p$  is the average position for the short molecular in-plane axis. The other short axis is perpendicular to the  $(n, p)$  plane.

Because of the tilt sign (+ or -) of the  $n$  director (Fig. 2 (b)) and two directions of the  $p$  polar director ( $+p$  and  $-p$ ) there are four different structures of  $B_2$  phase: 1. Synclinc ferroelectric ( $SmC_S P_F$ ) - the tilt angle is positive or negative in all smectic layers and  $p$  vectors are parallel, 2. Synclinc antiferroelectric ( $SmC_S P_A$ ), 3. Anticlinic ferroelectric ( $SmC_A P_F$ ), and 4. Anticlinic antiferroelectric ( $SmC_A P_A$ ). The last one shows up for two symmetric compounds (12OSOR and 14OSOR) studied in this work. A general symbol of  $B_2$  phase can be written as follows:  $SmC_{SA}P_{FA}$ , where index "S" stands for synclinc, A - for anticlinic order of molecules in two neighboring layers, F - for ferroelectric and A - antiferroelectric order of polarization vectors.

Banana-shaped compounds may form both lamellar and/or columnar mesophases (Szydłowska, 2003) that have become a subject of intensive experimental (Reddy & Tschierske, 2006) and theoretical studies (Vaupotič, 2006) in the last decades. In the first place research on electro-optic switching in ferro- and anti-ferroelectric phases composed of bent-core molecules has been done because of possible practical applications (Walba et al., 2000; Reddy & Tschierske, 2006).

Since the discovery of ferroelectric order in smectic B phases composed of polar achiral banana-shaped molecules many experimental studies have been done that confirm ferro- or antiferroelectric order inside the layers and positive (ferroelectric) or negative (antiferroelectric) correlations between the layers. Theoretical studies were focused on intermolecular interactions within the layers as well as interlayer correlations (Vaupotič & Čopič, 2005; Vaupotič, 2006).

Liquid crystalline materials built of bent-core molecules are also attractive because they exhibit new physical properties. They possess two-dimensional smectic phases that display qualitatively different physical properties than the calamitic ferroelectric liquid crystals (Pelzl, 1999; Reddy & Tschierske, 2006). Bent-core non-chiral molecules show tendency to form a polar order within the smectic layers. Using a dielectric spectroscopy method it was found (Kresse et al., 2001, Kresse, 2003) that the reorientation of polar molecules is strongly

hindered in  $B_2$  phase because of dense packing of bent-core molecules in smectic layers. Due to this the secondary order parameter (spontaneous polarization) is almost temperature independent.

Thin Langmuir-Blodgett films composed of bent-core molecules studied by reversal current method (Geivandov, 2006) reveal an interesting property that polarization of nano-layers is similar to bulk polarization. Both ferro- and anti-ferroelectric order have been observed. It was also found for nano-layers that the molecules are mobile in such restricted geometry what facilitates both ferro- and antiferroelectric switching.

Out of eight B phases:  $B_1$ ,  $B_2$ ,  $B_3$ , ...,  $B_7$ , and  $B_8$  (Reddy & Tschierske, 2006) the most thoroughly investigated seems to be the  $B_2$  phase which may show one of four types of order depending on the sign of tilt angle ( $+\theta$  or  $-\theta$ ) as well as on the sign of correlations (positive - ferroelectric order or negative - antiferroelectric order) between the polarization vectors of neighboring layers ( $\sim P_j \cdot P_{j+1}$ ). Complementary studies performed on a few homologous series show that compounds with shorter side chains ( $C_5 - C_9$ ) exhibit only a frustrated  $B_1$  phase, whereas those having longer chains ( $C_{10} - C_{14}$ ) generally display antiferroelectric  $B_2$  phase (Bedel et al., 2000).

The main objective of this article is to present dielectric and electro-optic behavior of  $B_1$  or  $B_2$  phases of four selected members of nOSOR series ( $n=8, 9, 12$  and  $14$ ). The first two show only  $B_1$  phase, and the other two with even number of carbon atoms in the side alkoxy chains display only  $B_2$  phase of  $SmC_{AP_A}$  type.

## 2. Experimental methods

To study phase transitions and physical properties of  $B_1$  and  $B_2$  phases the following complementary methods have been employed: DSC calorimetry, polarizing microscopy texture observation, linear dielectric spectroscopy, and reversal current method. Using the latter it was possible to record the reversal current spectra for the  $B_2$  phase in form of two well separated current peaks what substantiates antiferroelectric order of this phase. As also found, the  $B_1$  exhibits also some kind of ferroelectric order which is being gradually reduced upon temperature decreasing (Wierzejska-Adamowicz, 2010; Chruściel, 2011).

### 2.1 DSC calorimetric studies

Thermal properties of the substances investigated have been studied by differential scanning calorimetry using Pyris1 DSC made by Perkin Elmer Company. Transition temperatures and enthalpies of the transitions have been computed based on DSC heating and cooling thermograms. Fig. 3 presents DSC results for 8OSOR compound which possesses enantiotropic  $B_1$  phase showing up during cooling in a wide temperature range of 40 degrees. As one can see the melting process of this material is complex - on heating there are two transitions ( $Cr-Cr_2-Cr_1$ ) between solid modifications. Below the  $B_1$  enantiotropic phase there seems to be an orientationally disordered crystal (ODIC).

As an example endothermic and exothermic curves are shown in Fig. 4 for 12OSOR. It is seen that the  $B_2$  phase is also enantiotropic one. On heating two crystalline modifications ( $Cr_1$  and  $Cr_2$ ) were found. One should point out that all compounds studied in this work are thermally very stable - their clearing points do not change after a few heating and cooling runs.

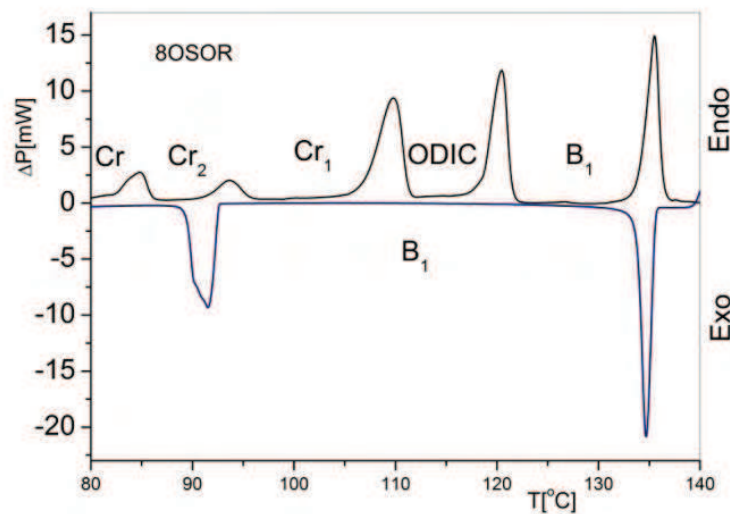


Fig. 3. Endothermic and exothermic runs obtained by Pyris 1 DSC for 8OSOR compound

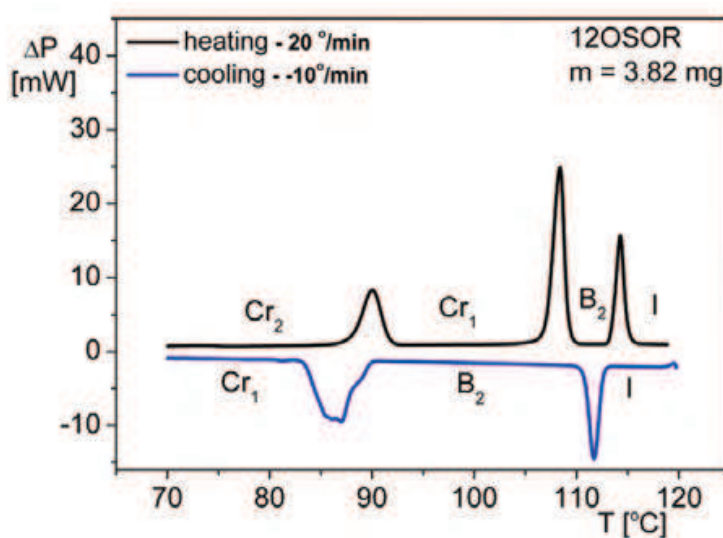


Fig. 4. DSC results obtained for 12OSOR compound on cooling and heating by using Pyris1 DSC

Studies of the physical properties of all compounds have been performed on cooling. The transition temperatures acquired by DSC method on cooling are as follows:

**8OSOR** - I 133.4 °C (16.9) → B<sub>1</sub> 92.7 °C (14.7) → Cr<sub>1</sub>

**9OSOR** - I 123.4 °C (16.0) → B<sub>1</sub> 82.6 °C (14.0) → Cr

**12OSOR** - I 112.6 °C (18.5) → B<sub>2</sub> 88.6 °C (38.7) → Cr<sub>1</sub>

**14OSOR** - I 114.6 °C (17.4) → B<sub>2</sub> 87.2 °C (57.6) → Cr

Transition enthalpies for the clearing and freezing points are given in round brackets in [kJ/mol]. As seen there are small differences between the clearing and freezing enthalpies for the first two homologs with B<sub>1</sub> phase.

## 2.2 Electro-optic methods

Texture observation and electro-optic switching between the planar and homeotropic textures for 12OSOR were done at LEMCEL using Olympus Polarizing Microscope BX60 and LINKAM temperature controller. Texture observations of 8OSOR, 9OSOR, 12OSOR, and 14OSOR were performed using Nikon Eclipse Polarizing Microscope LV100POL and INSTEC temperature controller in the Institute of Physics of the Jagiellonian University.

Polarizing microscopy measurements allowed us to identify phases and to observe a planar inhomogeneous (Fig. 5(a)) and homeotropic textures of  $B_2$  phase. The homeotropic texture (Fig. 6 (a)) was observed after applying bias field equal to  $26 \text{ V}_{\text{p-p}} / \mu\text{m}$ . Figs. 5 (b) and 6 (b) present schematic molecular arrangements of the local planar and homeotropic alignments, respectively. Due to the splay deformation (Takanishi, 2003; Vaupotic, 2005) the texture is planar inhomogeneous (quasi-planar) with characteristic circular domains (Fig. 5 (a)). Under strong electric field ( $26 \text{ V}_{\text{p-p}} / \mu\text{m}$ ) a fast transition to homeotropic texture is observed with secondary optical axis being perpendicular to the electrodes. Using triangular driving field at a certain voltage value a completely black homeotropic state was observed. Similar electro-optic behavior has been found for 14OSOR (Wierzejska-Adamowicz, 2010, Wierzejska-Adamowicz et al., 2010).

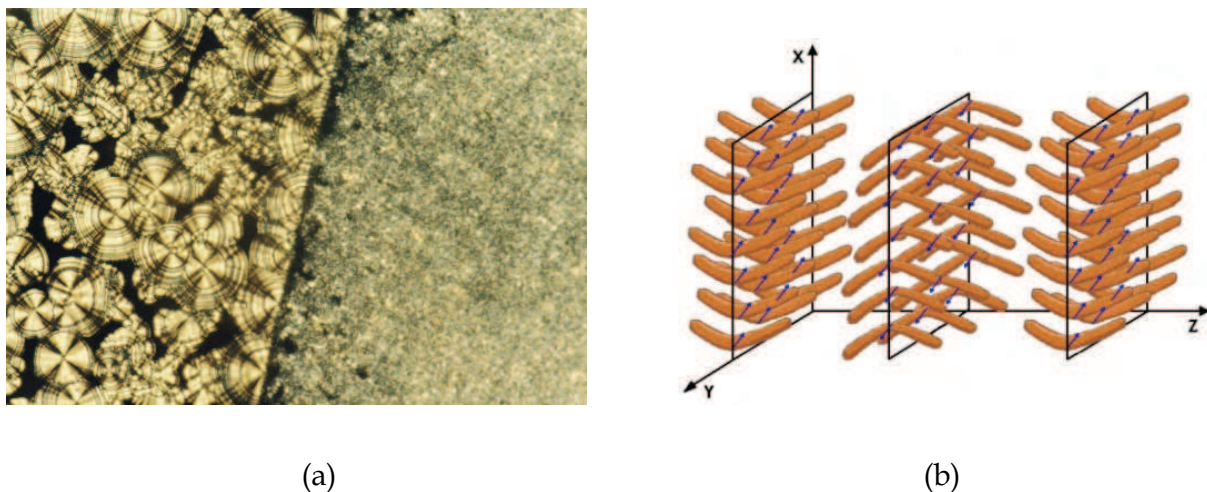


Fig. 5. (a) Planar texture of 12OSOR's  $B_2$  phase obtained at  $T=116.8^\circ\text{C}$ ,  $U=0 \text{ V}_{\text{p-p}}/\mu\text{m}$ , AWAT HG cell -  $d=1.7 \mu\text{m}$  and (b) schematic local alignment of molecules in planar  $B_2$  phase.

This shows undoubtedly that there is an electro-optic switching between the two states  $\text{SmC}_{\text{AP}_A} \rightarrow \text{SmC}_{\text{S}_F}$ . Upon applying triangular voltage wave the extinction directions of the characteristic circular domains (Fig. 5 (a)) reorient clockwise or counterclockwise depending on the field direction what was observed for symmetric (Walba et al., 2000; Sadashiva et al., 2000; Zhang et al., 2006) and asymmetric (Lee et al., 2010) banana-shaped systems. However, it was not possible to grow a mono-domain of uniform planar alignment even upon applying strong electric fields. Inhomogeneous planar texture (Fig. 5 (a)) was, consisting of Maltese crosses originated from concentric layer structures, was observed. Such structures were revealed by X-ray diffraction (Takanishi, 2003). Characteristic brushes forming Maltese crosses (Ortega et al., 2004) coincide with the polarizer-analyzer positions due to anticlinic order of molecules in two neighboring layers forming a pseudo-unit cell. The authors were able to grow  $B_2$  phase after applying a strong electric field to  $B_1$  phase.

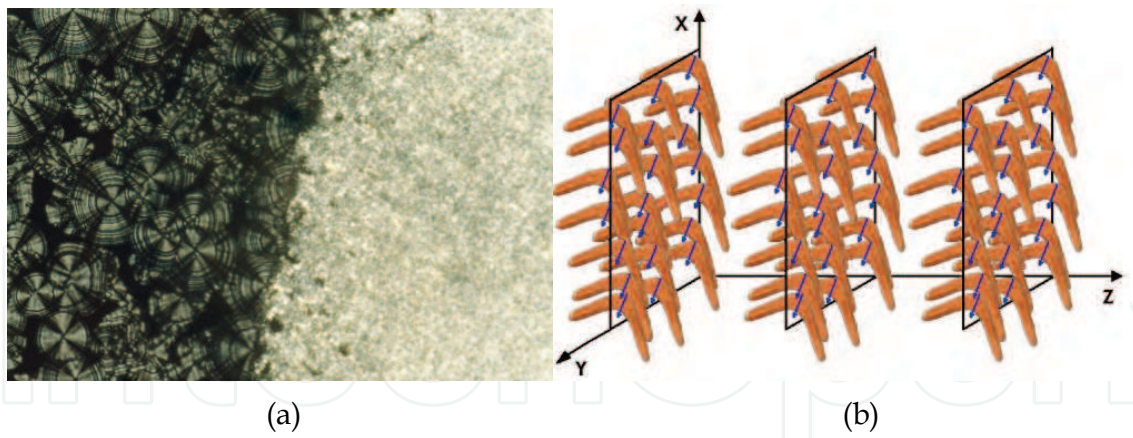


Fig. 6. (a). Quasi-homeotropic texture of 12OSOR's  $B_2$  phase observed at  $T=116.8^\circ\text{C}$ ,  $U=26\text{ V}_{\text{p-p}}/\mu\text{m}$ , AWAT HG cell -  $d=1.7\ \mu\text{m}$  and (b) schematic local alignment of molecules in homeotropic  $B_2$  phase. Electric field is parallel to the X-axis. It is worth pointing out that upon applying triangular voltage wave a completely black state (homeotropic) was observed at a certain voltage value.

It is worth noting that the characteristic mosaic texture of  $B_1$  phase does not change at all under A.C. field and electro-optic switching is not observed (Ossowska-Chruściel, D.M. et al., 2007; Wierzejska-Adamowicz, 2010). Spontaneous polarization measurements were carried out - by means of reversal current method - using  $1.7\ \mu\text{m}$  and  $3.2\ \mu\text{m}$  AWAT HG ITO cells for 9OSOR and 12OSOR, respectively. The experimental set-up consists of

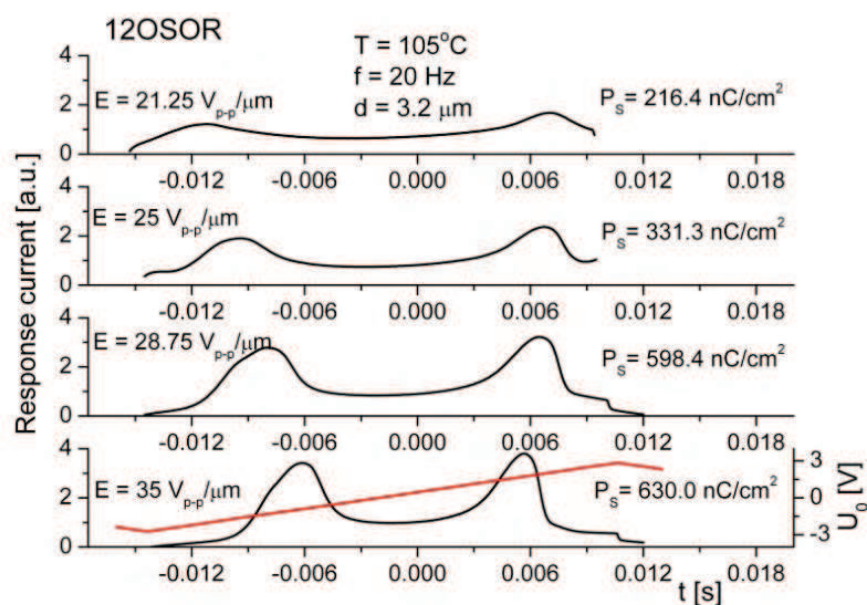


Fig. 7. Reversal current peaks obtained for antiferroelectric  $B_2$  phase of 12OSOR at different driving voltages - from threshold to saturation voltage (see also Fig. 9). The real value of the driving voltage was equal to  $U_0 \times 20\text{ V}_{\text{p-p}}$

Agilent 3310A wave form generator, FLC Electronics amplifier F20ADI and digital scope Agilent DSO6102A.

The  $B_2$  phases of 12OSOR and 14OSOR compounds are antiferroelectric ( $\text{SmC}_A\text{P}_A$ ), so after applying to the electrodes a triangular wave two peaks are observed as

the current response of the sample in half a period of the driving voltage (Fig. 7). As seen in Fig. 8 spontaneous polarization of 12OSOR is very high - it reaches a value close to 600 nC/cm<sup>2</sup> and is weakly temperature dependent in the B<sub>2</sub> phase. The measurements were done applying driving electric field of 35 V<sub>p-p</sub>/μm and frequency of 20 Hz. Spontaneous polarization of 14OSOR is slightly smaller and its temperature dependence is also weak (Chruściel, 2011)

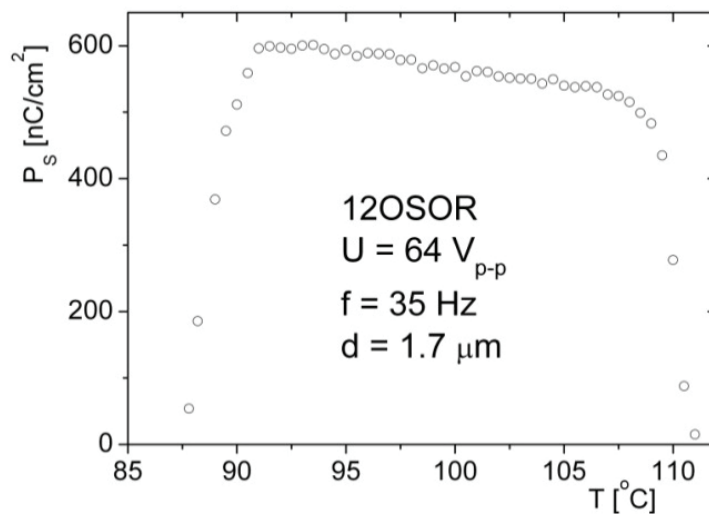


Fig. 8. Spontaneous polarization of B<sub>2</sub> phase vs. temperature for 12OSOR compound

As seen in Fig. 9 the polarization of B<sub>2</sub> phase depends non-linearly on electric field. Above 30V<sub>p-p</sub>/μm it becomes saturated reaching the value of spontaneous polarization. In addition this non-linear dependence begins above the threshold field (ca. 21 V<sub>p-p</sub>/μm at 110 °C)

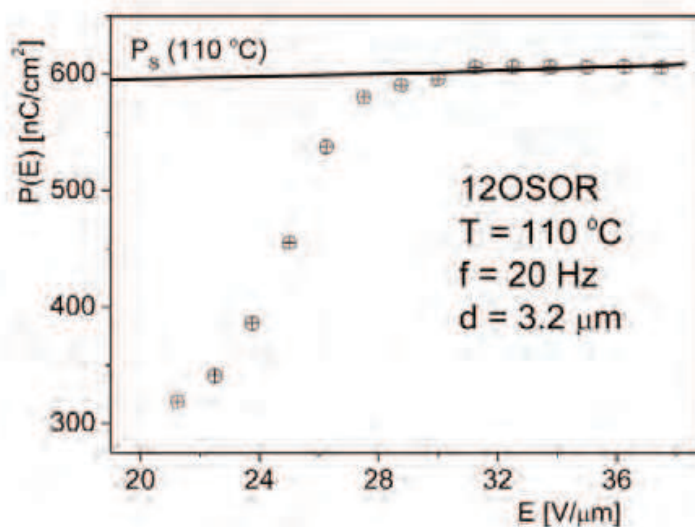


Fig. 9. Polarization vs. electric field of 12OSOR's B<sub>2</sub> phase at selected temperature of 110 °C

As seen in Figs. 8 and 9 the B<sub>2</sub> phase of 12OSOR exhibits large spontaneous polarization. As found before the B<sub>2</sub> phases composed of bent-core asymmetric molecules (Kohout et al., 2010) show distinctly smaller spontaneous polarization (from 200 to 380 nC/cm<sup>2</sup>) but upon cooling ferroelectric - antiferroelectric transition was observed.

As known, in  $B_1$  phase the side alkoxy chains of the molecules in one layer overlap on the cores of molecules in neighboring layers and there is a compensation of microscopic polarization (Reddy & Tschierske, 2006). However, using strong electric field one can induce polarization in this phase (Figs. 10 and 12) due to positive short range order of dipole moments inside the layers.

The  $B_1$  phase of 9OSOR shows a reasonable reversal current response (Fig. 10) which is typical for switching polarization vector from  $+P_s$  to  $-P_s$  in ferroelectrics. However, the temperature dependence of spontaneous polarization (Fig. 11) is not like that for a ferroelectric or antiferroelectric phase of classical ferroelectric liquid crystals (Wróbel et al., 2003). It can be treated as an induced polarization originating from molecular polar clusters created due to steric interactions inside the layers. It decreases with temperature decreasing due to inter- and/or intra-layer negative dipole-dipole correlation which are stronger at low temperatures.

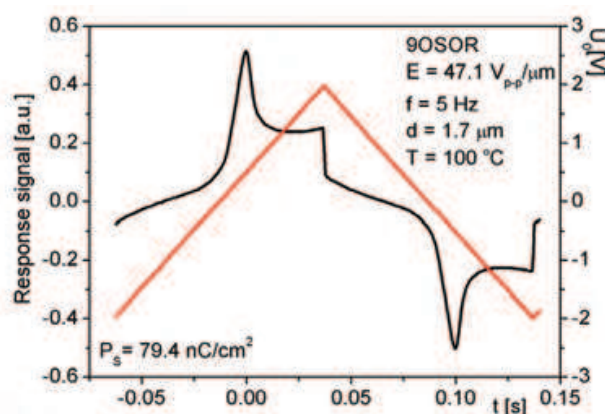


Fig. 10. Triangular driving voltage (right-hand side scale) applied vs. time and reversal current spectrum (left-hand side scale) of  $B_1$  phase of 9OSOR acquired for  $E = 47.1 \text{ V}_{p-p}/\mu\text{m}$ ,  $f = 5 \text{ Hz}$ ,  $d = 1.7 \mu\text{m}$  and at  $T = 100^\circ\text{C}$ . The real value of the driving voltage was equal to  $U_0 \times 20 \text{ V}_{p-p}$

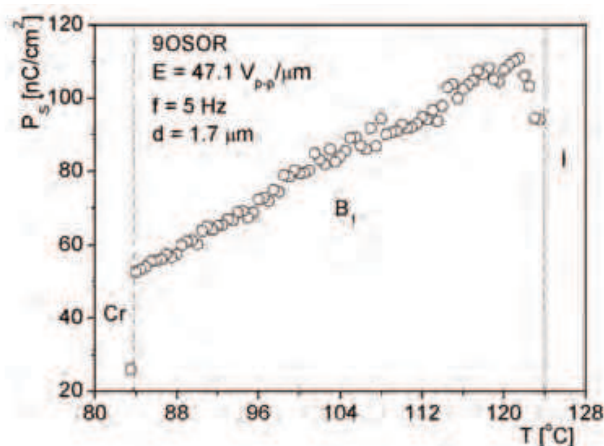


Fig. 11. Polarization of 9OSOR's ferroelectric  $B_1$  phase vs. temperature. Measurement conditions: triangular voltage wave -  $E = 47.1 \text{ V}_{p-p}/\mu\text{m}$ ,  $f = 5 \text{ Hz}$ ,  $d = 1.7 \mu\text{m}$

As found before by the dielectric relaxation spectroscopy, in the  $B_1$  phase there exists antiparallel dipole-dipole correlation of transverse dipole moments (Kresse et al., 2001; Kresse, 2003). There is also a strong retardation of molecular reorientational motions at the I- $B_1$  (or  $B_2$ )

phase transition which is being caused by high order of bent-core molecules in B phases. Large value of the transition enthalpies for the transition between the isotropic and liquid crystalline phase of these materials as well as weak temperature dependence of the spontaneous polarization of B<sub>2</sub> phase also substantiate high order of B phases. As one can additionally notice the enthalpy changes of melting and freezing points (Figs. 3 and 4) are distinctly smaller than those obtained for calamitic liquid crystals what reflects a distinctly smaller change of order between liquid crystalline and crystalline phase of bent-core systems.

It has been found in this study that the polarization of B<sub>1</sub> phase changes non-linearly with electric field applied (Fig. 12) yet it does not reach such large values as those obtained for the B<sub>2</sub> phase. Like for B<sub>2</sub> phase (Fig. 9) there is a threshold field of ca. 12 V/μm, above which a single reversal current peak shows up (Fig. 10), and above 25 V/μm the polarization of B<sub>1</sub> phase saturates but its value is smaller than 120 nC/cm<sup>2</sup>. This effect is most probably due to short range ferroelectric order and/or modulated structures (Szydłowska, 2003).

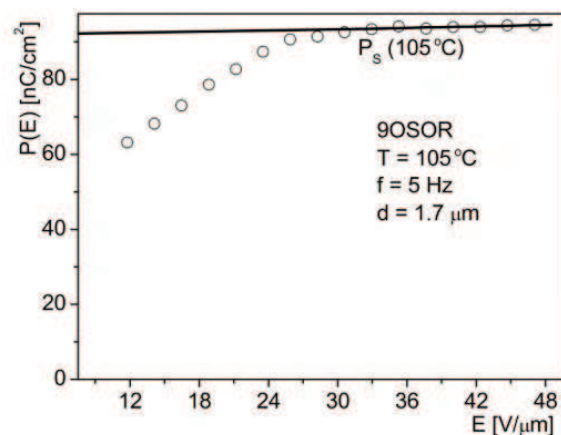


Fig. 12. Polarization vs. electric field applied to the sample of 9OSOR's ferroelectric B<sub>1</sub> phase. Parameters: frequency of the driving voltage -  $f = 5$  Hz, thickness of the sample  $d = 1.7$  μm.

### 2.3 Dielectric spectroscopy

Dielectric measurements were done using dielectric spectrometer based on Agilent 4294A precision impedance analyzer controlled by PC using a program written on VisualStudio.NET platform. Substances were put by means of capillary action into HG - 5μm AWAT cells with gold electrodes. The dielectric spectrometer allows one to measure dielectric spectra with high accuracy. The measurements have been done using the cells with gold electrodes covered with rubbed polymer layers what facilitates planar but for banana-shaped molecules inhomogeneous alignment. The dielectric spectra were acquired in the frequency range from 40 Hz to 25 MHz. More than 60 experimental points were acquired per one frequency decade. Bias field was used to align the biaxial B<sub>2</sub> phase so that the polar director  $p$  is perpendicular to the electrodes. The B<sub>2</sub> is a biaxial phase having the dielectric permittivity tensor of the form:

$$\hat{\epsilon}^*(\omega) = \begin{pmatrix} \epsilon_{11}^*(\omega) & 0 & 0 \\ 0 & \epsilon_{12}^*(\omega) & 0 \\ 0 & 0 & \epsilon_{11}^*(\omega) \end{pmatrix} \quad (1)$$

In this study it was possible to measure two principal components of this tensor, namely  $\varepsilon_{\perp 1}^*(\omega)$  and  $\varepsilon_{\perp 2}^*(\omega)$ , where the latter was measured along the secondary optical axis. The difference:

$$\varepsilon_{\perp 2} - \varepsilon_{\perp 1} = \delta\varepsilon \quad (2)$$

can be treated as a measure of biaxiality (Lagerwall, 1998) of the B<sub>2</sub> phase. It has been shown by means of the dielectric spectroscopy (Ossowska-Chruściel et al., 2009; Wierzejska-Adamowicz et al., 2010; Chruściel, 2011) that with electric measuring fields being parallel to the polar director  $p$  one observes an enhanced dielectric absorption and electric permittivity as well. As found in scope of this work there is an asymmetry of the dielectric spectra between the positive and negative bias fields (Fig. 13 (a) and (b)). It means that the system studied has low point symmetry. B phases composed of bow-shaped molecules may exhibit one of the following low point symmetries:  $C_{2v}$ ,  $C_{2h}$ ,  $C_2$  and even  $C_1$  (Pelzl et al., 1999).

Exemplary dielectric spectra – obtained vs. bias field - are presented in Figs. 13 (a) and (b). As seen there is an asymmetry of the dielectric spectra – the intensity of dielectric absorption depends on the sign of bias voltage. The dielectric absorption of the high frequency dielectric relaxation process is distinctly larger for negative bias fields. On the other hand, the low frequency dielectric relaxation process is being stronger enhanced for positive than negative bias fields (Fig. 13 (a)).

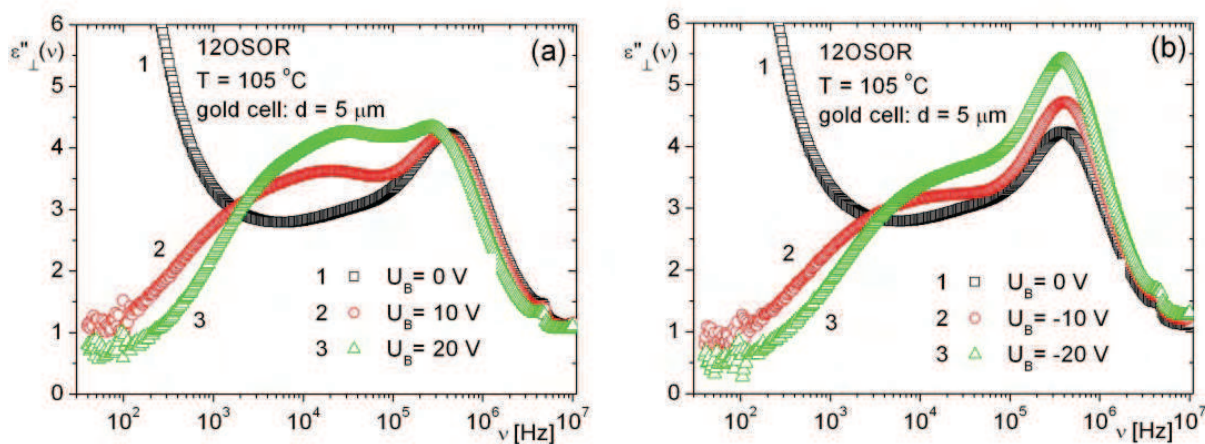


Fig. 13. Bias field dependences of dielectric spectrum measured for B<sub>2</sub> phase of 12OSOR. (a) Dielectric spectra for positive and (b) negative bias voltages

The B<sub>2</sub> phase is biaxial with the director  $n$  and polar director  $p$ . Using strong electric fields it was possible to observe in A.C. electric field transitions between a quasi-planar and homeotropic state with polar director  $p$  being normal to the electrodes. Using our HG gold cells and the experimental conditions it was not possible to study the dielectric spectrum of the B<sub>2</sub> phase aligned homeotropically with primary director  $n$  being parallel to electric measuring field.

### 2.3.1 Bias field influence

The dielectric spectra were processed by using ORIGIN 7.0 software. The following complex function was fit to the experimental points measured without bias field:

$$\varepsilon_{\perp 1}^*(\omega) = \varepsilon_{\perp 1}(\infty) + \frac{\varepsilon_{\perp 1}(0) - \varepsilon_{\perp 1}(\infty)}{1 + (i\omega\tau)^{1-\alpha}} - \frac{i\sigma_{\perp 1}}{\varepsilon_0 v^M} + \frac{B}{v^N}, \quad (3a)$$

where  $\varepsilon_{\perp 1}(\infty)$  is a high frequency electric permittivity,  $\varepsilon_0$  - electric permittivity of the free space,  $\varepsilon_{\perp 1}(0)$  - static electric permittivity for planar alignment due to surface interaction,  $\tau$  - dielectric relaxation time,  $\alpha$  - distribution parameter of relaxation times ( $0 \leq \alpha \leq 1$ ),  $\sigma_{\perp 1}(\omega)$  - ionic conductivity,  $\omega = 2\pi\nu$  is a circular frequency and  $B, M, N$  - phenomenological fitting parameters. The last term in Eq. (3a) originates from electrode polarization effect. By fitting Eq. (3a) to the experimental points acquired without bias field (Fig. 14), the following dielectric parameters have been obtained:  $\varepsilon_{\perp 1}(\infty) = 3.78$ ,  $\varepsilon_{\perp 1}(0) = 13.51$ . The latter can be treated as the static dielectric constant for planar alignment. All fitting parameters are given in Fig. 14. In the low frequency range there are contributions to the dielectric relaxation spectrum coming from ionic conductivity and a sub-hertz relaxation process for the  $M$  parameter is distinctly smaller than 1.

Because the experimental dielectric spectra obtained under different bias fields for homeotropic alignment consist of two relaxation processes, the following complex fitting function was used for data analysis:

$$\varepsilon_{\perp 2}^*(\omega) = \varepsilon_{\perp 2}(\infty) + \frac{\varepsilon_{\perp 2}(01) - \varepsilon_{\perp 2}(\infty)}{1 + (i\omega\tau_2)^{1-\alpha_2}} + \frac{\varepsilon_{\perp 2}(0) - \varepsilon_{\perp 2}(01)}{1 + (i\omega\tau_1)^{1-\alpha_1}}, \quad (3b)$$

where  $\varepsilon_{\perp 2}(\infty)$  is a high frequency electric permittivity,  $\varepsilon_{\perp 2}(0)$  - static electric permittivity for homeotropic alignment,  $\varepsilon_{\perp 2}(01)$  - quasi-static electric permittivity,  $\tau_1$  and  $\tau_2$  - are relaxation times,  $\alpha_1$  and  $\alpha_2$  - distribution parameters of relaxation times, ( $0 \leq \alpha_i \leq 1, i = 1, 2$ ), and  $\omega = 2\pi\nu$  is a circular frequency. One should explain that in Eq. (3b) the conductivity and polarization electrode terms were omitted because bias fields suppress the ionic contribution to the dielectric spectra (see Figs. 15 and 22).

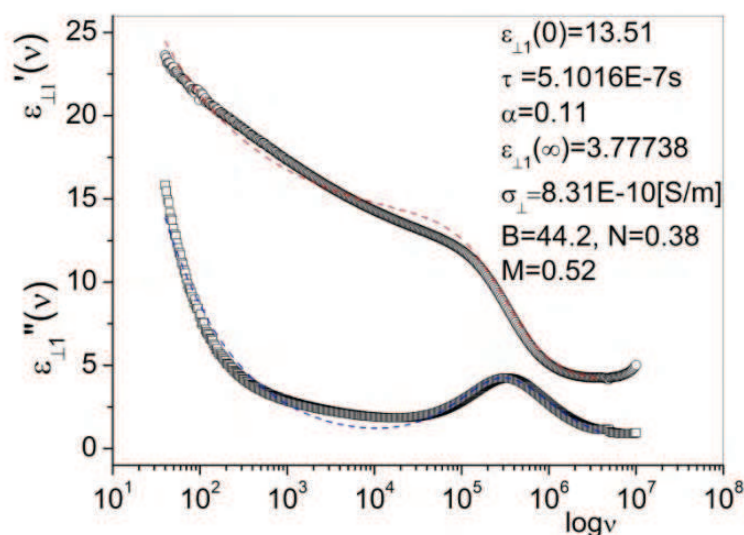


Fig. 14. Dielectric spectrum of antiferroelectric B<sub>2</sub> phase of 12OSOR obtained for planar alignment (without bias voltage) at T=95°C. Dispersion and absorption curves (dashed lines) were obtained by fitting Eq. (3a) to the experimental points.

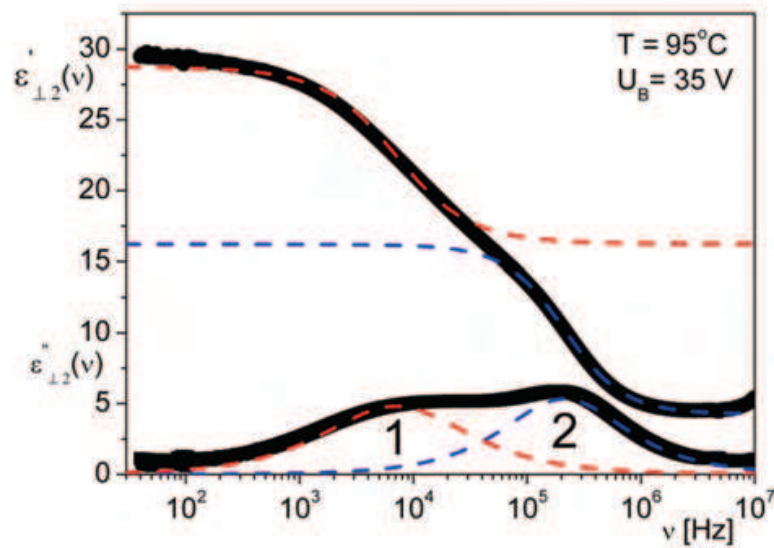


Fig. 15. Dielectric spectrum of antiferroelectric B<sub>2</sub> phase of 12OSOR obtained with bias voltage (homeotropic alignment). Dispersion and absorption curves (dashed lines) were obtained by fitting Eq. (3b) to the experimental points.

T = 95 °C					
U <sub>B</sub> [V]	Process 1/2	ε <sub>i</sub> (0)	τ <sub>i</sub> [s]	α <sub>i</sub>	ε <sub>i</sub> (∞)
U <sub>B</sub> = 35	1	29.84	1.6 E-5	0.36	12.67
	2	12.67	6.78 E-7	0.02	4.23
U <sub>B</sub> = 30	1	30.45	1.88 E-5	0.35	12.55
	2	12.55	6.83 E-7	0.03	4.23
U <sub>B</sub> = 25	1	31.77	1.84 E-5	0.38	11.32
	2	11.32	6.37 E-7	0.01	4.16
U <sub>B</sub> = 20	1	32.68	1.8 E-5	0.42	9.96
	2	9.96	5.8 E-7	-0.04	4.07
U <sub>B</sub> = 15	1	33.63	1.93 E-5	0.46	9.04
	2	9.04	5.39 E-7	-0.08	3.93
U <sub>B</sub> = 10	1	34.40	2.23 E-5	0.49	8.86
	2	8.86	5.18 E-7	-0.10	3.77
U <sub>B</sub> = 5	1	34.49	2.54 E-5	0.52	9.52
	2	9.52	5.07 E-7	-0.09	3.62

Table 1. Dielectric parameters vs. bias voltage obtained by fitting Eq. (3b) to the dielectric spectra measured at different positive bias voltages

T = 95 °C					
$U_B$ [V]	Process 1/2	$\epsilon_i(0)$	$\tau_i$ [s]	$\alpha_i$	$\epsilon_i(\infty)$
$U_B = -35$	1	30.73	1.56 E-5	0.35	13.62
	2	13.62	6.54 E-7	0.01	4.22
$U_B = -30$	1	30.97	1.5 E-5	0.36	13.47
	2	13.47	6 E-7	0.01	4.18
$U_B = -25$	1	31.08	1.7 E-5	0.37	13.43
	2	13.43	5.69 E-7	0.01	4.16
$U_B = -20$	1	31.32	1.9 E-5	0.39	12.99
	2	12.99	5.45 E-7	0.01	4.13
$U_B = -15$	1	31.96	2.13 E-5	0.42	11.96
	2	11.96	5.22 E-7	-0.02	4.06
$U_B = -10$	1	32.88	2.35 E-5	0.46	11.02
	2	11.02	5.07 E-7	-0.04	3.94
$U_B = -5$	1	34.13	2.66 E-5	0.51	10.35
	2	10.35	5.02 E-7	-0.07	3.74

Table 2. Dielectric parameters vs. bias voltage obtained by fitting Eq. (3b) to the dielectric spectra measured at different negative bias voltages

### 3. Results and discussion

Dielectric spectra of the aligned by electric field  $B_2$  phase consists of two relaxation processes (Fig. 16) which can be ascribed to the molecular reorientation (2) and the collective fluctuations (1) of ferroelectric domains, respectively.

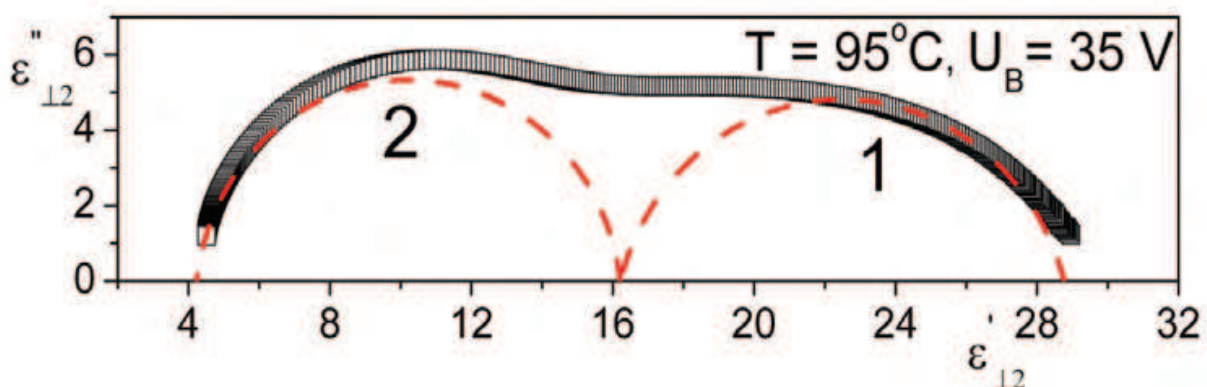


Fig. 16. Cole-Cole plot of the dielectric spectrum obtained at the highest bias field for 12OSOR's antiferroelectric  $B_2$  phase. Dashed lines were obtained by fitting Eq. (3b) to the experimental points.

The high frequency dielectric relaxation (2) is a Debye-type process originated from the reorientation of molecules around their long axes (see Fig. 2 (a)). Its Cole-Cole plot is a semicircle with the centre lying on the  $\epsilon'_{\perp 2}$  axis. However, the numerical splitting of the complex spectrum is not fully unique as for high bias fields the  $\alpha_2$  distribution parameter has small but negative (unphysical) values (Tables 1 and 2). Figs. 17, 18 and 19 present, respectively, bias field dependences of the relaxation times, distribution parameters and boundary electric permittivities. All these Figs. as well as Fig. 13 show some asymmetry in bias field dependence of physical quantities measured for the B<sub>2</sub> phase. The low frequency dielectric relaxation process (1) exhibits a distribution of the relaxation times characterized by the  $\alpha_1$  parameter that decreases with bias field increasing (Fig. 18, Tables 1 and 2). The static electric permittivity ( $\epsilon_{\perp 2}(0)$ ) is being enhanced after application of small bias field but it decreases with D.C. bias field (Fig. 13) which may be due to partial suppression of the collective mode connected with modulated structure of the B<sub>2</sub> phase.

It is worth noting here that the low frequency dielectric dispersion ( $\epsilon'$ ) and absorption ( $\epsilon''$ ) are affected by ionic conductivity. In calamitic LCs the adequate contribution to the dielectric absorption is usually described by the well know term:  $\sigma/(\epsilon_0\omega)$ . As found for bow-shaped systems (Schmalfuss et al., 1999; Kresse et al., 2001, Chruściel et al., 2011) this term should be modified by introducing the  $M$  parameter (Eq. (3a)) to obtain better agreement between theory and experiment. The main reason for such a difference is merging of pure ionic contribution with the low frequency dielectric relaxation (or relaxations) originated from fluctuations of modulated (or undulated) polarization vectors.

One should notice that the Goldstone mode in classical ferroelectric liquid crystals is usually a Debye-type relaxation process characterized by a single relaxation time (Wróbel et al., 2003). Modulated structures in B phases cause a distribution of the relaxation times what is reflected in the large value of the  $\alpha_1$  parameter ( Fig. 18, Table 1 and 2)

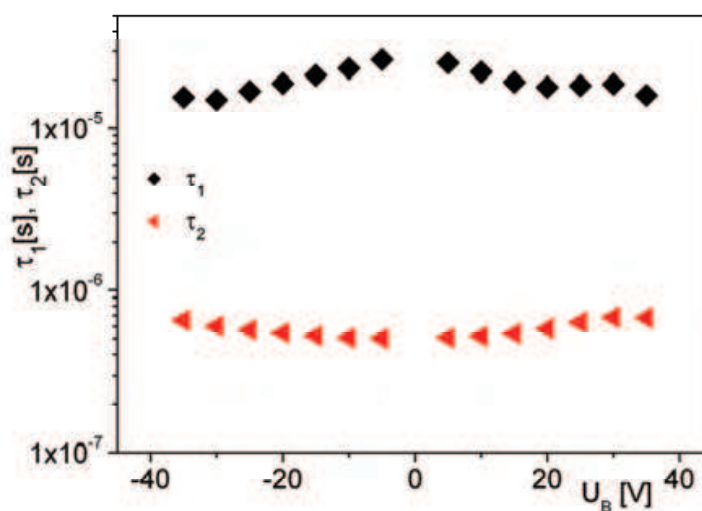


Fig. 17. Collective ( $\tau_1$ ) and molecular ( $\tau_2$ ) dielectric relaxation times obtained by fitting Eq. (3b) to the experimental dielectric spectra vs. bias field

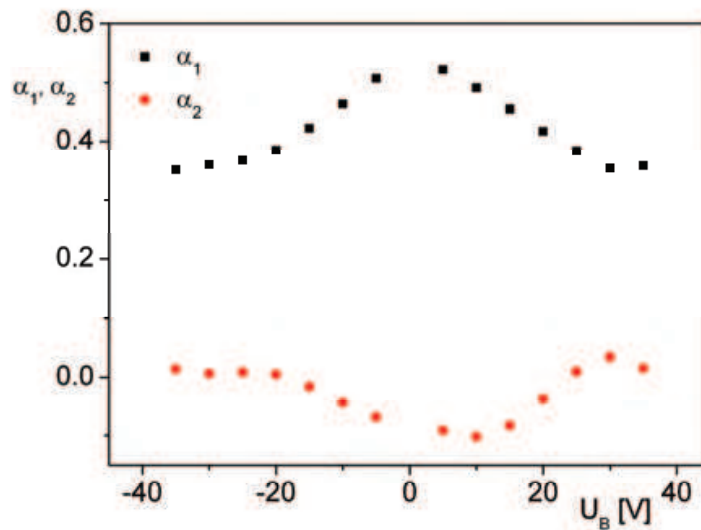


Fig. 18. Distribution parameters of molecular ( $\alpha_2$ ) and collective ( $\alpha_1$ ) relaxation processes obtained by fitting Eq. (3b) to the experimental dielectric spectra vs. bias field

### 3.2 Biaxiality of antiferroelectric $B_2$ phase

Fig.19 presents two static electric permittivities ( $\epsilon_{\perp 2}(0)$  and  $\epsilon_{\perp 2}(01)$ ) measured on the homeotropically aligned sample and vs. bias field. The values of  $\epsilon_{\perp 2}(0)$  and  $\epsilon_{\perp 2}(01)$  obtained at the highest bias voltages ( $U_B = \pm 35V$ ) seem to refer to homeotropic alignment.

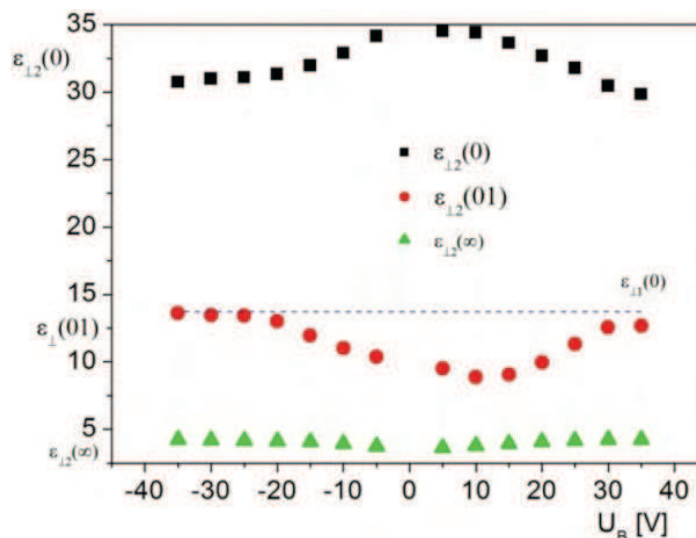


Fig. 19. Boundary electric permittivities vs. bias field computed for two principal directions by fitting Eqs. (3a) and (3b) to the experimental points

The value of  $\epsilon_{\perp 1}(0) = 13.51$ , represented in Fig. 19 by the dashed line, corresponds to the static electric permittivity obtained for planar alignment – without bias field. As seen in Fig. 19 the biaxiality of  $B_2$  given by Eq. (2) is positive for positive bias at low frequencies ( $\delta\epsilon_1=16.33$ ) and negative ( $\delta\epsilon_2=-0.84$ ) above the frequencies higher than  $10^5$  Hz ( $1/\tau_1$ ). For negative bias field both these values are positive:  $\delta\epsilon_1=17.25$  and  $\delta\epsilon_2=0.11$ . It is due to asymmetry of the electric permittivity tensor (Eq. (1)).

### 3.3 Dielectric relaxation processes of B<sub>1</sub> phase

As found the dielectric spectra of molecular origin measured for B<sub>1</sub> phases of 8OSOR (Ossowska-Chruściel et al., 2007) and 9OSOR (Wierzejska-Adamowicz et al., 2010) do not depend on bias fields. Fig. 20 shows 3D graphs of the dielectric absorption measured without (a) and with (b) bias field for 9OSOR compound. As seen the adequate dielectric spectrum obtained with a D.C. bias is practically the same. In both cases only one relaxation process shows up and it is connected with molecule reorientation around the short axis which is perpendicular to the vectors  $n$  and  $p$  (Fig. 2 (a)). The activation energy obtained without bias field (Fig. 21) is equal to  $\Delta E=112$  kJ/mol which is typical value for reorientation around the short molecular axis. However, in the papers published before by other authors (Kresse et al., 2001) this process is interpreted as reorientation around the long molecular axis which is on the average parallel to the director  $n$  (Fig. 2 (a)).

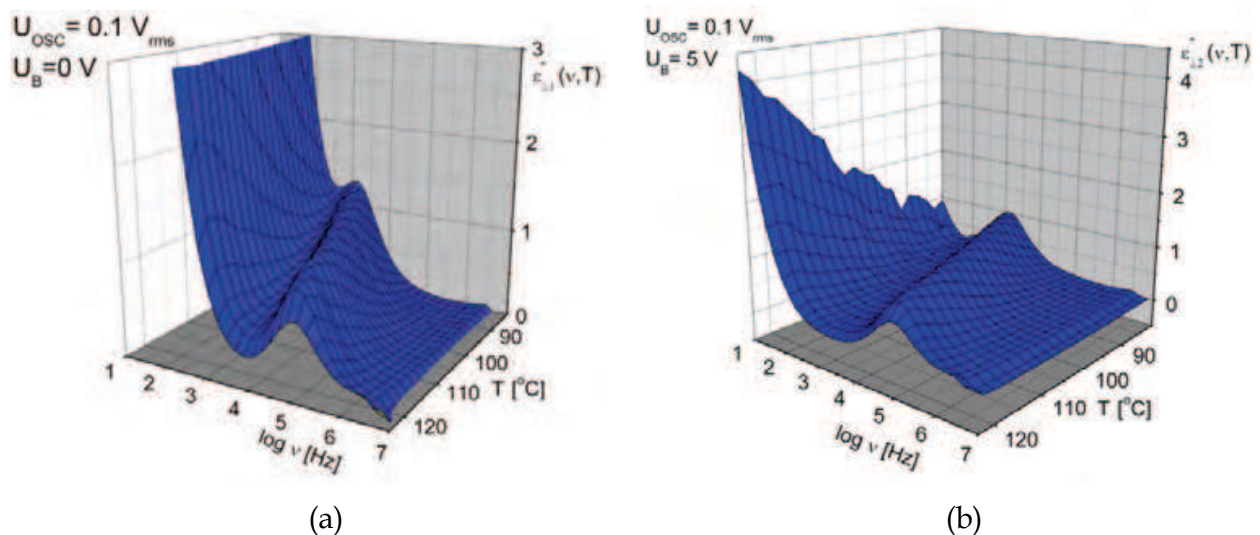


Fig. 20. Dielectric loss vs. frequency for B<sub>1</sub> phase in 9OSOR – (a) without bias field, (b) with bias field

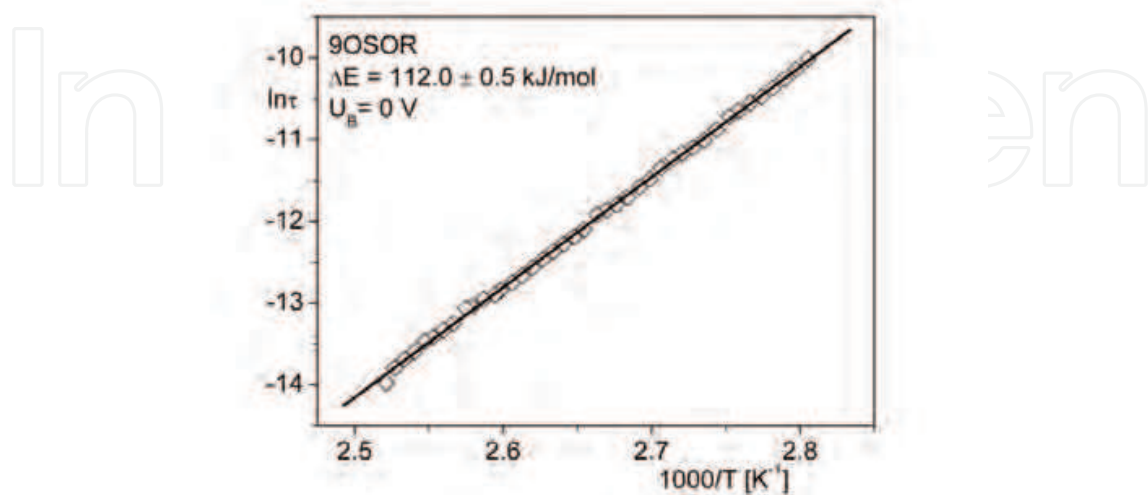


Fig. 21. Arrhenius plot for the dielectric relaxation process for B<sub>1</sub> phase observed without bias field

Similar dielectric relaxation spectrum was obtained before (Kresse, 2003; Ossowska-Chruściel, 2007). Our interpretation of the dielectric relaxation process observed in the  $B_1$  phase is based on the value of activation energy as well as on possible rectangular columnar structure of such phases (Sadashiva, 2000) what facilitates the reorientation around one of the short axes.

### 3.4 Dielectric relaxation processes of $B_2$ phase

Fig. 22 presents 3D graphs of the dielectric absorption spectra acquired without (a) and with (b) bias voltage equal to 15 V for 12OSOR compound. As seen the dielectric spectra measured with bias field show two well separated relaxation processes (see also Figs. 15 and 16) on the contrary to the  $B_1$  phase of 9OSOR which shows only one dielectric relaxation process. In the low frequency range the relaxation process is connected with fluctuations of ferroelectric domains showing up clearly in homeotropic structure of the  $B_2$  phase. The relaxation process observed in the high frequency range, appearing also without bias field, is connected with the molecule reorientation around the long axis. For 12OSOR the dielectric spectrum appears to be more complex: in the high temperature range of  $B_2$  phase it is connected with molecule reorientation around short molecular axis, whereas in the low temperature range – around the long axis (Wierzejska-Adamowicz, 2010). The activation barrier of the process connected with fluctuations of domains is equal to  $\Delta E=62$  kJ/mol (Fig. 23), whereas for the process connected with reorientation around long axis it is about 45 kJ/mol for measurements with and without bias field (Wierzejska-Adamowicz, 2010). The activation barrier found for reorientation around short molecular axis – observed in a narrow temperature range below the clearing point - is equal  $\Delta E=102$  kJ/mol (Wierzejska-Adamowicz, 2010).

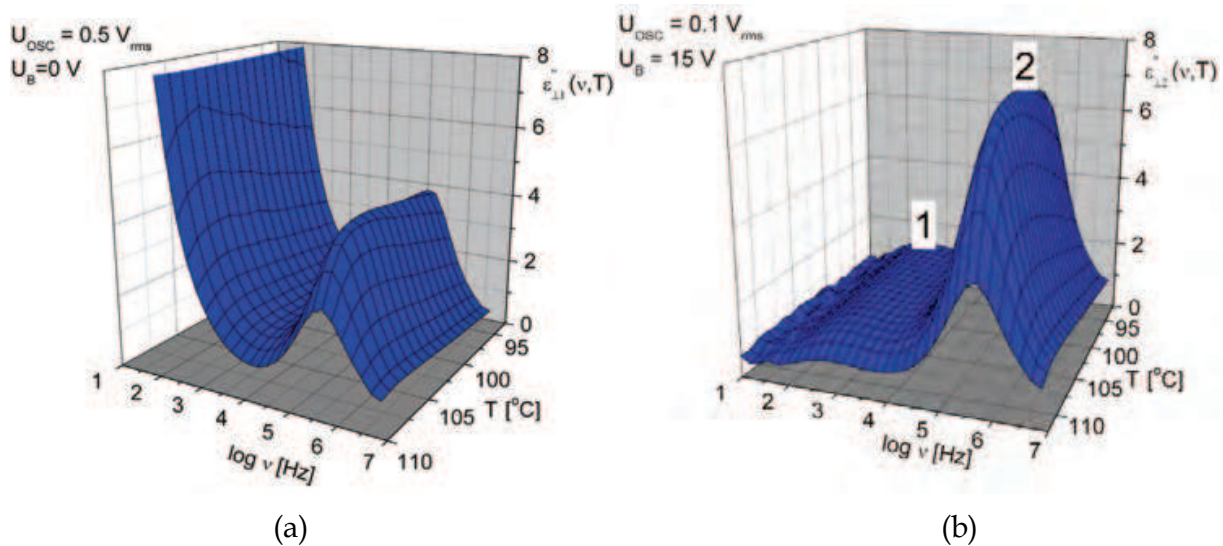


Fig. 22. 3D plot of dielectric loss vs. frequency for  $B_2$  phase of 12OSOR – (a) Without bias field, (b) With bias field

To sum up one should say the following: in B phases of bent-core systems the molecular rotational motions are slowed down due to strong steric interactions inside the layers. This effect is also substantiated by NMR studies (Domenici et al., 2006) where evidences of extremely slow rotational dynamics of bent-core molecules have been found.

As the  $\epsilon_{\perp 2}(\infty)$  is quite large and close to 4.0 (Fig. 19, Table 1 and 2), one should expect fast dielectric relaxation processes in the microwave frequency range. Intra-molecular reorientations of linear mesogenic units (Fig. 2 (a)) around their long axes and reorientations of the alkoxy chains contribute to electric permittivity at high frequencies.

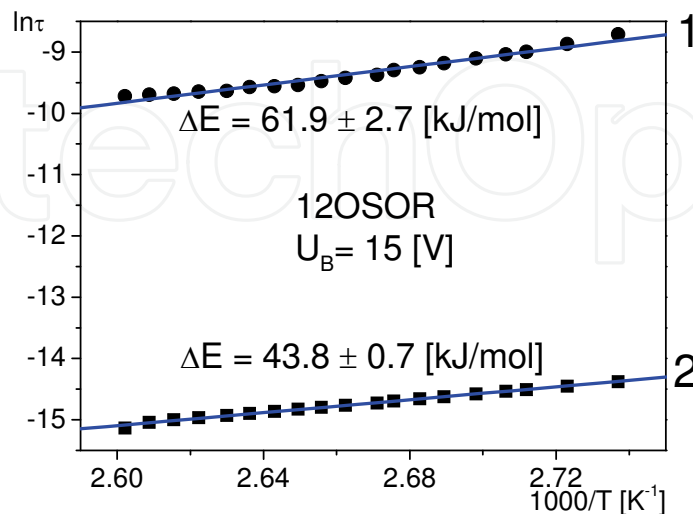


Fig. 23. Arrhenius plot for the two dielectric relaxation processes of the  $B_2$  phase studied under bias field

#### 4. Conclusions

Our studies show that  $B_1$  phase of 9OSOR does not exhibit any low frequencies dielectric relaxation of collective nature. Under strong electric fields  $B_1$  phase shows polarization which is due to short range ferroelectric order inside the smectic layers. This polarization linearly decreases with temperature decreasing. On the other hand, it displays non-linear dependence on electric field what is typical for ferroelectrics.

On the contrary 12OSOR and 14OSOR having even number of carbon atoms in alkoxy side chains exhibit anticlinic and antiferroelectric  $SmC_A P_A$  phase showing both collective and molecular dielectric relaxation processes. Two principal components ( $\epsilon_{\perp 1}^*(\omega)$  and  $\epsilon_{\perp 2}^*(\omega)$ ) of the dielectric permittivity tensor show qualitatively different dielectric relaxation spectra of this biaxial phase.

The  $B_2$  phase is biaxial with the primary director  $n$  and polar secondary order parameter  $p$ . Using strong electric fields, it was possible to observe a fast electro-optic switching between a quasi-planar and homeotropic state with polar director  $p$  being normal to the electrodes.

The dielectric spectroscopy studies on two principal alignments of the  $B_2$  phase shed some light upon the structure and dynamics of this phase.

#### 5. Acknowledgments

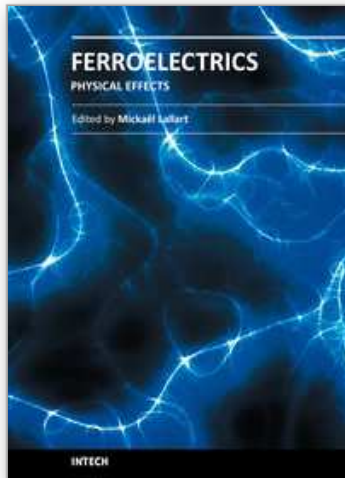
Financial support of the State Committee for Scientific Research (KBN) in scope of the grant No. N N202 076435 is gratefully acknowledged.

The research was carried out with the equipment purchased thanks to the financial support of the European Regional Development Fund in the framework of the Polish Innovation Economy Operational Program (contract no. POIG.02.01.00-12-023/08).

## 6. References

- Bedel, J. P., Rouillon, J. C, Marcerou, J. P., Laguerre, M., Achard, M. F. & Nguyen, H. T. (2000). Physical characterization of B<sub>1</sub> and B<sub>2</sub> phases in a newly synthesized series of banana shaped molecules. *Liq. Crystals*, Vol. 27, No. 1, pp. 103-113
- Chruściel, J., Wierzejska-Adamowicz, M., Ossowska-Chruściel, D. M., Marzec, M., Wawrzyniak, A., Douali, R., Legrand, Ch. & Wróbel, S. (2011). Dielectric Spectroscopy of Bent-core Thioesters' B Phases. *Mol. Cryst. & Liq. Cryst.* Vol. 541, pp. 490-499
- Domenici, V., Fodor-Csorba, K., Frezzato, D., Moro, G., & Veracini, C. A. (2006). Deuterium NMR Evidence of Slow Dynamics in the Nematic Phase of Banana-Shaped Liquid Crystals. *Ferroelectrics*, Vol. 344, pp. 19-28
- Geivandov, A. R., Palto, S.P. Yudin, S. G., Blinov, L. M., Pelzl, G. & Weissflog, W.(2006). Ferro- and Atiferroelectric Properties of Langmuir-Blogett Films Composed of Bent-Core Molecules. *Ferroelectrics*, Vol. 344, pp. 3-10
- Kohout, M., Chambers, M., Vajda, A., Galli, G., Domjan, A., Svoboda, J., Bubnov, A., Jakli, A. & Fodor-Csorba, K. (2010). Properties of non-symmetric bent-core liquid crystals with variable flexible chain length. *Liq. Crystals*, Vol. 37, pp. 537-545
- Kresse, H., Schmalfuss H., Weissflog, W., Tschierske, C. & Hauser, A. (2001). Dielectric Characterization of B<sub>n</sub> Phase. *Mol. Cryst. and Liq. Cryst.*, Vol. 366, pp. 505-517
- Kresse, H. (2003). Chap. 5.7, In: *Relaxation Phenomena*, Eds. W. Haase and S. Wróbel, pp. 400-422, ISBN 3-540-44269-3, Springer-Verlag, Berlin-Heidelberg-New York
- Lagerwall, S.(1998),Chap. 2, In: *Handbook of Liquid Crystals*. Vol. 2B: *Low molecular weight liquid crystals*. Eds. D. Demus, J.W. Goodby, G.W. Gray, H.W. Spiess & V. Vill, pp.513-664, ISBN 3-527-29502-X, WILEY-VCH Verlag, GmbH, D-60469 Weinheim (Federal Republic of Germany)
- Lee, S. K., Kang, S., Tokita, M. & Watanabe, J. (2010). Formation of homochiral antiferroelectric ground state in asymmetric bent-shaped achiral molecules. *Liq. Cryst.*, Vol. 37, No. 5, pp. 593-598
- Liang, H.-H. & Lee, J.-Y. (2011). Enhanced enantiotropic B<sub>2</sub> phase by mixing homologous chlorine-substituted molecules. *Liq. Crystals*, Vol. 38, No. 2, pp. 163-167
- Link, D.R., Natale, G., Shao, R., Maclennan, J.E., Clark, N.A., Körblova, E., Walba, D. M. (1997). Spontaneous Formation of Macroscopic Chiral Domains in a Fluid Smectic Phase of Achiral Molecules. *Science*. Vol. 278, pp. 1924-1927
- Noiri, T., Sekine, T., Watanabe, J., Furukawa, T. & Takezoe, H. (1996). Distinct ferroelectric smectic liquid crystals consisting of banana shaped achiral molecules. *J. Mater. Chem.* Vol. 6, No. 7, pp. 1231-1233
- Ortega, J., de la Fuente, M.R., Etxebarria, Folcia, C.L., Diez, S., Gallastegui, J.A., Gimeno, N., Ros, M.B. & Pérez-Jubindo, M.A. (2004). Electric-field-induced B<sub>1</sub>-B<sub>2</sub> transition in bent-core mesogens. *Phys. Rev. E*, Vol. 69, 011703-1(7)
- Ossowska-Chruściel, D.M., Kudłacz, K., Sikorska, A., Chruściel, J., Marzec, M., Mikułko, A., Wróbel, S., Douali, R. & Legrand, Ch. (2007). Ferroelectric properties of achiral banana-shaped and calamitic chiral thioesters. *Phase Transit.* Vol. 80, pp. 781-
- Ossowska-Chruściel, D. M., Wierzejska-Adamowicz, M., Marzec, M., Mikułko, A., Douali, R., Legrand, Ch., Chruściel, J., Sikorska, A. & Wróbel, S. (2009). Planar-Homeotropic Transition Observed for B<sub>2</sub> Phase of Banana-Shaped Thioester. *Phase Transit.* Vol. 82, No. 12, pp. 889-898

- Pelzl, G., Diele, S. & Weissflog, W. (1999). Banana-Shaped Compounds - A New Field of Liquid Crystals. *Adv. Mater.* Vol. 11, No. 9, pp.707-724
- Reddy, R. A. & Tschierske, C. (2006). Bent-core liquid crystals: polar order, superstructural chirality and spontaneous desymmetrisation in soft matter systems. *J. Mater. Chem.* Vol. 16, pp. 907-961
- Rouillon, J., Marcerou, J., Laguerre, M., Nguyen, H. & Achard, M. (2001). New banana-shaped thiobenzoate liquid crystals with B<sub>6</sub>, B<sub>1</sub> and B<sub>2</sub> phases. *J. Mater. Chem.* Vol. 11, 2946-2950
- Sadashiva, B.K., Raghunathan, V.A., Pratibha, R. (2000). Evidence of Columnar Structure ion Compounds Composed of Banana-Shaped Molecules, *Ferroelectrics*, Vol. 243, pp. 249-260
- Schmalfuss, H., Shen, D., Tschierske, C. & Kresse, H. (1999). Dielectric investigations of the B<sub>2</sub> phase. *Liq. Crystals*, Vol. 26, 1767
- Sekine, T., Takanishi, Y., Noiri, T., Watanabe, J. & Takezoe, H. (1997). Ferroelectric Properties in Banana-Shaped Liquid Crystalline Systems. *Jpn. J. Appl. Phys.*, Vol. 36, L1201-L1203
- Szydłowska, J., Mieczkowski, J., Matraszek, J., Bruce, D.W., Górecka, E., Pocięcha, D. & Guillon, D. (2003). Bent-core liquid crystals forming two- and three-dimensional modulated structures. *Phys. Rev. B*, Vol. 67, pp.031702-1(5)
- Takanishi, Y., Ogasawara, T., Ishikawa, K., & Takezoe, H., Watanabe, J., Takahashi, Y. & Iida, A. (2003), Local layer structures in circular domains of an achiral bent-core mesogen observed by X-ray microbeam diffraction. *Phys. Rev E*, Vol. 68, pp. 011706-1(5)
- Vaupotič, N. & Čopič, M. (2005). Polarization modulation instability in liquid crystals with spontaneous symmetry breaking, *Phys. Rev. E*, Vol. 72, 031701-1(4)
- Vaupotič, N. (2006). Landau-de Gennes Theory of the Polarization Modulated and Layer Undulated Structure in Liquid Crystals Made of Bent-Core Molecules. *Ferroelectrics*, Vol. 344, pp.151-159
- Walba, D. M., Körblova, E., Shao, Maclennan, J.E., R., Link, D.R., Glaser, M.A. & Clark, N.A. (2000). A Ferroelectric Liquid Crystal Conglomerate Composed of Racemic Molecules. *Science*. Vol. 288, pp. 2181-2184
- Wierzejska-Adamowicz, M., Ossowska-Chruściel, D. M., Marzec, M., Mikułko, A., Chruściel, J., Douali, R., Legrand, Ch. & Wróbel, S. (2010). Electrooptic and dielectric investigations of frustrated B1 phase and antiferroelectric B2 phases of banana-shaped thioesters. *Acta Phys. Polonica*, Vol. 117, pp. 557-561
- Wierzejska-Adamowicz, M., Ossowska-Chruściel, D. M., Czerwiec, J., Marzec, M., Mikułko, A., Chruściel, J., Douali, R., Legrand, Ch. & Wróbel, S. (2010). Bias field influence on dielectric spectra of B phases of bent-core thioesters. *Optical Review*, Vol. 17, pp.393-398
- Wierzejska-Adamowicz, M. (2010), *Ph D Thesis*, Jagiellonian University, Kraków 2010
- Wróbel, S., Haase, W., Kilian, D., Chien, L.-C. & Chong-Kwang, L. (2000). High Temperature Antiferroelectric Smectic Phase Composed of Banana-Shaped Achiral Molecules", *Ferroelectrics*, Vol. 243, pp. 277-289
- Wróbel, S., Haase, W., Fafara, A. & Marzec, M. (2003). Chap. 5.11, In: *Relaxation Phenomena*, Eds. W. Haase and S. Wróbel, pp. 485-510, ISBN 3-540-44269-3, Springer-Verlag, Berlin-Heidelberg-New York
- Zhang, Y., Wand, M., O'Callaghan, M.J., Walker, Ch. M. & Thurmes, W. (2006). Anticlinic Ferroelectric Bananas for Electro-optic Modulators. *Ferroelectrics*, Vol. 344, pp. 11-18



## **Ferroelectrics - Physical Effects**

Edited by Dr. Mickaël Lallart

ISBN 978-953-307-453-5

Hard cover, 654 pages

**Publisher** InTech

**Published online** 23, August, 2011

**Published in print edition** August, 2011

Ferroelectric materials have been and still are widely used in many applications, that have moved from sonar towards breakthrough technologies such as memories or optical devices. This book is a part of a four volume collection (covering material aspects, physical effects, characterization and modeling, and applications) and focuses on the underlying mechanisms of ferroelectric materials, including general ferroelectric effect, piezoelectricity, optical properties, and multiferroic and magnetoelectric devices. The aim of this book is to provide an up-to-date review of recent scientific findings and recent advances in the field of ferroelectric systems, allowing a deep understanding of the physical aspect of ferroelectricity.

### **How to reference**

In order to correctly reference this scholarly work, feel free to copy and paste the following:

Stanisław Wróbel, Janusz Chruściel, Marta Wierzejska-Adamowicz, Monika Marzec, Danuta M. Ossowska-Chruściel, Christian Legrand and Redouane Douali (2011). Ferroelectric Liquid Crystals Composed of Banana-Shaped Thioesters, *Ferroelectrics - Physical Effects*, Dr. Mickaël Lallart (Ed.), ISBN: 978-953-307-453-5, InTech, Available from: <http://www.intechopen.com/books/ferroelectrics-physical-effects/ferroelectric-liquid-crystals-composed-of-banana-shaped-thioesters>

**INTECH**  
open science | open minds

### **InTech Europe**

University Campus STeP Ri  
Slavka Krautzeka 83/A  
51000 Rijeka, Croatia  
Phone: +385 (51) 770 447  
Fax: +385 (51) 686 166  
[www.intechopen.com](http://www.intechopen.com)

### **InTech China**

Unit 405, Office Block, Hotel Equatorial Shanghai  
No.65, Yan An Road (West), Shanghai, 200040, China  
中国上海市延安西路65号上海国际贵都大饭店办公楼405单元  
Phone: +86-21-62489820  
Fax: +86-21-62489821

© 2011 The Author(s). Licensee IntechOpen. This chapter is distributed under the terms of the [Creative Commons Attribution-NonCommercial-ShareAlike-3.0 License](#), which permits use, distribution and reproduction for non-commercial purposes, provided the original is properly cited and derivative works building on this content are distributed under the same license.

IntechOpen

IntechOpen